



10 – 12 may, Aveiro, Portugal

SiF'06

Fourth International Workshop Structures in Fire

Taken from the proceedings page 837 – 849

FIRE RESISTANCE OF HIGH-STRENGTH CONCRETE-FILLED STEEL COLUMNS

PETER SCHAUMANN¹, VENKATESH KODUR² and OLIVER BAHR³

ABSTRACT

At ambient temperature, the load-bearing capacity of Hollow Structural Section steel columns can be improved by using high strength concrete as filling. However, it is difficult to predict the behavior of high strength concrete in case of fire because of complex phenomena like micro cracking and spalling. A numerical investigation with the computer program BoFIRE, verified by comparison to test data, was undertaken to investigate if the high strength concrete material properties given by the North American and European codes lead to a reliable prediction of the fire resistance period. Different types of high strength concrete-filling are considered. Furthermore, Eurocode 2 provides a simplified approach for the determination of the fire resistance period of concrete-filled Hollow Structural Section steel columns. Since it is restricted to normal strength concrete-filling, it is examined if the range of application can be extended to high strength concrete-filling.

1. INTRODUCTION

The filling of Hollow Structural Section (HSS) steel columns with high strength concrete (HSC) offers many advantages over traditional columns at room temperature. The enhanced load-bearing capacity allows minimized dimensions of the cross-section and hence more usable space in buildings. In contrast to this, the filling with HSC may cause problems at elevated temperatures in case of fire. Due to its reduced porosity, which is equal to small and less interconnected pores, HSC is sensitive to rising temperatures since water cannot evaporate. The build-up of steam-pressure may lead to micro cracks and spalling because of the low tensile strength of concrete. This results in a sharply reduced fire resistance period.

¹ Professor, University of Hannover, Institute for Steel Construction, Hannover, Germany,
email: schaumann@stahl.uni-hannover.de.

² Professor, Michigan State University, Department of Civil and Environmental Engineering, East Lansing, USA, email: kodur@egr.msu.edu.

³ Research Assistant, University of Hannover, Institute for Steel Construction, Hannover, Germany,
email: bahr@stahl.uni-hannover.de.



A numerical study is performed using the Finite Element-based computer program BoFIRE to investigate the behavior of HSS steel columns filled with HSC at elevated temperatures. The European¹ and North American^{2,3} code provisions for material properties and load computations are implemented in the computer program. The validity of the material properties is established by comparing predictions from the model with test data published in the literature. It included three different types of filling with plain HSC, steel fiber reinforced HSC and bar reinforced HSC.

2. TESTING PROGRAM

A review of literature indicates that there is very limited fire tests on HSC-filled HSS columns exposed to fire^{4,5}. The main objective of the reported tests was to determine the fire resistance of HSS steel columns filled with different types of HSC. The tests, that were undertaken on HSS columns, included plain HSC-filling (columns C-46 and C-47), HSC with steel fibers (columns C-36 and SQ-11) and HSC with 4×15 mm reinforcement bars (column SQ-14), and is presented in Figure 1. Full details of the fire tests are documented in references [4] and [5].

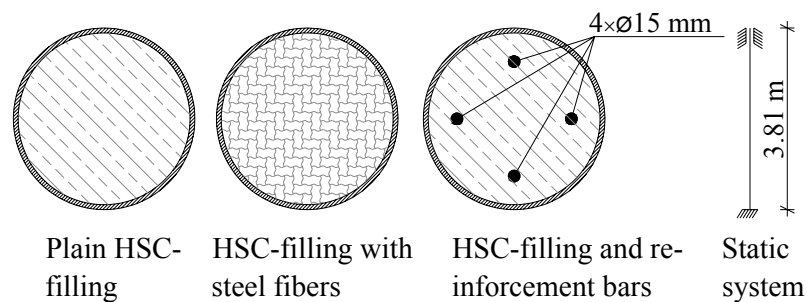


Fig. 1 – Cross-section and static system of circular HSC-filled HSS columns.

The tested HSS columns were 3.81 m long with fixed-fixed end conditions and filled with calcareous (limestone) HSC. After the load was applied, the columns were exposed to heating according to the Canadian code CAN/ULC-S101-M89⁶ until failure occurred. This fire is equivalent to ASTM E-119 or ISO-834 standard fire. The fire resistance period of some of the tested columns (selected from literature) is calculated with the computer program BoFIRE. This allows verification of material properties given by the North American and European codes. Moreover, it facilitates to study the influence of the concrete filling on the fire resistance. The material properties for steel fiber reinforced HSC-filling are taken according to the published data by Kodur & Sultan⁷, which is reproduced in the appendix. The test data of the different columns, taken from references^{4,5,17}, is summarized in Table 1, where the ‘C’ in the column denotes circular cross-section and ‘SQ’ square cross-section.

Tab. 1 – Summary of fire resistance test data on HSC-filled HSS columns^{4,5,17}.

| Tube filling | Column | Cross-section | Test load in kN | Concrete strength in MPa | Fire resistance in minutes |
|--------------------|--------|---------------|-----------------|--------------------------|----------------------------|
| Plain HSC | C-46 | 273.1 x 6.35 | 1,050 | 82.2 | 48 |
| | C-47 | 273.1 x 6.35 | 1,050 | 107.0 | 51 |
| Steel fibers | C-36 | 219.1 x 4.78 | 600 | 98.1 | 174 |
| | SQ-11 | 203.2 x 6.35 | 900 | 99.5 | 128 |
| Reinforcement bars | SQ-14 | 203.2 x 6.35 | 1,150 | 81.7 | 89 |



3. SIMPLIFIED APPROACH ACCORDING TO EUROCODE 2, PART 1-2¹

The Eurocode 4, part 1-2⁸ is relevant for the design of composite structures. However, this code only provides tabular data for the fire design of concrete-filled HSS columns. The corresponding annex also offers the possibility of computing the residual load-bearing capacity in case of fire. For this purpose it is necessary to determine the temperature field which is elaborate. Apart from these two methods, this code refers to the Eurocode 2, part 1-2¹ for fire design of concrete structures. Provided that the steel tube is neglected, it is allowed to use the so-called simplified Method A from the latter code. The advantage is that this method is based on a simple formula. However, the equation is restricted to normal strength concrete. A comparison of fire resistance predictions from the Eurocode equation with test results (see Table 1) is undertaken to investigate if the scope of application can be extended to HSC-filled HSS columns.

It should be noted that the studied columns C-46, C-47, C-36 and SQ-11 are not within the scope of application since a minimum of four reinforcement bars is required which they do not have. Therefore these columns were assumed to have four bars. Yet this does not result in higher fire endurance according to Method A. The concrete cover was set to 25 mm, leading to a negative impact on the fire resistance so that the result can be seen as conservative. As regards the columns SQ-11 and SQ-14, it has to be stated that the restriction of the parameter 'b' is not kept. Since the discrepancy is rather small, these columns were also examined with the simplified approach. The outcome of the investigation is presented in Figure 2.

With respect to the columns C-46 and C-47 with mere HSC-filling, the fire resistance period calculated by the simplified Method A is close to the corresponding test result. This is in as far astonishing as these columns do not provide the reinforcement bars which is a precondition for the use of the simplified approach.

For the HSS steel columns C-36 and SQ-11, with steel fiber reinforced concrete filling, the approach computes very conservative results, which is underlined by Figure 2. This can be attributed to the fact that Method A does only take conventional reinforcement into account, but not the beneficial effect of steel fibers. The result for the column SQ-14 with reinforcement bars is conservative, too.

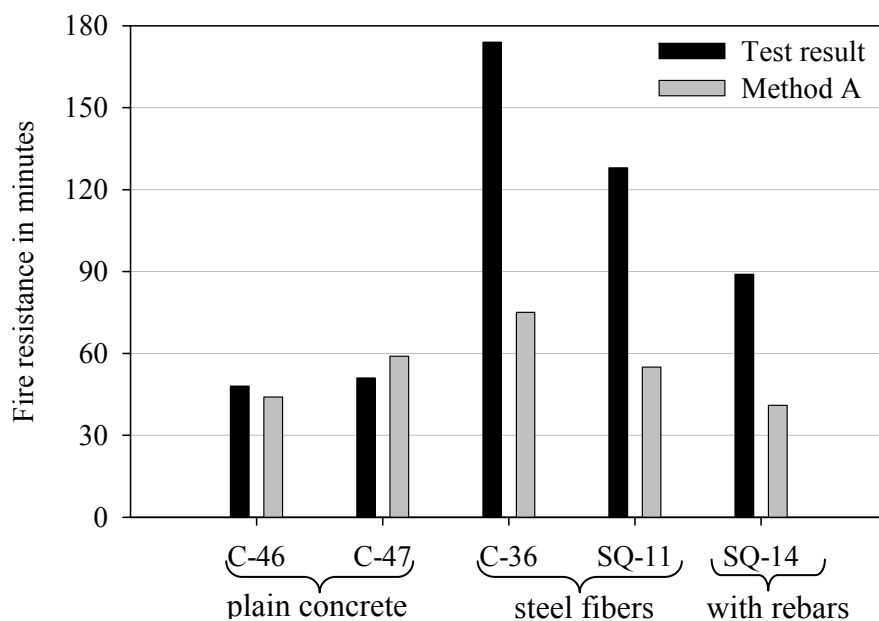


Fig. 2 – Comparison between tested and calculated fire resistance.



4. PRESENTATION OF THE USED FEM-PROGRAM BOFIRE

All parametric studies were carried out using the transient, non-linear, incremental computer code BoFIRE. This program was written by Schaumann⁹ and further developed by Upmeyer¹⁰ and Kettner¹¹. It is capable of predicting thermal and structural behavior of both steel and composite structures exposed to fire. The program is based on the following principle:

$$R(t) \geq S(t) \quad (1)$$

where $R(t)$ = resistance at time t ; $S(t)$ = effect of mechanical action at time of fire exposure t .

The load-bearing capacity of structures $R(t)$, which are charged by a mechanical load $S(t)$ while exposed to fire, depends on the modification of the material properties, such as decreasing of strength and elastic modulus affected by heat. Thus, the procedure for determining the remaining load-bearing capacity of structures is based on a numerical calculation model coupling the thermal and mechanical response at various time steps. At first, the thermal response takes place. In this stage, the fire temperature and the temperature distribution of the cross-section are computed. According to the temperature distribution, the modification of the material properties caused by temperature can be computed. Subsequently, the mechanical response is calculated where deformation and remaining strength of the members are determined. These results are compared to the applied load on the column and it is verified whether the structure still has sufficient load-bearing capacity. This procedure is repeated for various time steps until the resistance of the member is less than the applied load, which represents failure of the column. The duration to failure is taken as the fire resistance period of the column.

4.1 Thermal response

In BoFIRE, the temperature field is calculated using the Fourier differential equation for heat conduction:

$$-div(\lambda \times grad \theta) + c \times \rho \times \dot{\theta} - f = 0 \quad (2)$$

where λ = thermal conductivity; θ = temperature; c = heat capacity; ρ = density; $\dot{\theta}$ = derivation of temperature with respect to time; f = heat source.

Caused by the modifications of material properties due to heat exposure, the differential equation becomes transient since the temperature field gets inhomogeneous. Thus, that equation has to be solved numerically. In the following, the basis of that method will be described according to Kettner¹¹. A mathematical transformation of Equation (2) results in the weak formulation of the differential equation:

$$\int_{\Omega} \lambda \times grad \theta : grad \delta\theta dA + \int_{\Gamma} q \times \delta\theta \times n dS + \int_{\Omega} \rho \times c \times \dot{\theta} \times \delta\theta dA = 0 \quad (3)$$

where Ω = area; Γ = boundary of considered area; q = heat flux; n = normal vector on the boundary.



For the solution of the weak form, bi-linear shape functions on a four node isoparametric element according to Equation (4) are used.

$$N_i = \frac{1}{4} \times (1 \pm \eta) \times (1 \pm \xi) \quad (4)$$

The approach is presented on the left side of Figure 3. An example for mesh generation with BoFIRE is shown at the right side of Figure 3. Moreover, the computer program BoFIRE also recognizes different material properties as a function of temperature including that of fire protection materials.

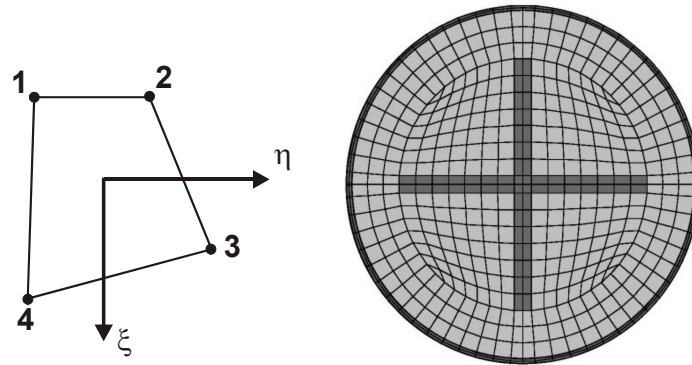


Fig. 3 – Four node isoparametric element (left) and mesh for a concrete-filled HSS column with embedded X-shape profile (right).

4.2 Mechanical response

It is possible to calculate all types of cross-sections and linear structures as beams, columns or plane frames taking second order theory into account. The calculation is based on the Bernoulli hypothesis for plain state of strains. Shear deformations are not considered. Due to the nonlinear material properties, cross-sectional values and internal forces depend on the temperature field and strains into the cross-section. The strains are calculated by the balance of internal and external forces. The solution of the incremental system equation is given by Schaumann⁹:

$$\Delta \underline{S}_L - \Delta \underline{S}_{th} = (\underline{K}_t^I - \underline{K}_{t_0}^I) \times \underline{v}_{t_0} + \Delta \underline{K}^{II} \times \underline{v}_{t_0} + (\underline{K}_t^I + \underline{K}_t^{II}) \times \Delta \underline{v} \quad (5)$$

where $\Delta \underline{S}_L$ = difference between external forces per time increment; $\Delta \underline{S}_{th}$ = difference between thermal strains per time increment; $(\underline{K}_t^I - \underline{K}_{t_0}^I) \times \underline{v}_{t_0}$ = difference of system matrix stiffness (elastic portion); $\Delta \underline{K}^{II} \times \underline{v}_{t_0}$ = difference of system matrix stiffness (geometric portion according to second order theory); $(\underline{K}_t^I + \underline{K}_t^{II}) \times \Delta \underline{v}$ = difference of deformations per time increment.

At first, the internal force variables and deformations caused by the external forces $\Delta \underline{S}_L$ are computed in one or more increments. In a parallel calculation the temperature field is established as previously described. Because of the incremental procedure it is possible to linearize the influence of non-linear material behavior and temperature distribution.



5. COMPARISON BETWEEN TESTED AND COMPUTED FIRE RESISTANCE

The tested and calculated fire resistance period of the different columns can be seen in Figure 4. A moisture content of 10% was considered in the computer program BoFIRE. Regarding the numerical results for HSS columns filled with plain HSC it is obvious that the fire resistance is overestimated to a great extent. This is true for both the North American and the European HSC material properties. With respect to the circular HSS columns C-46 and C-47 it is obvious that the gap between the tested and calculated fire endurance becomes greater with increasing concrete compressive strength. However, the results for both numerical models are conservative for HSC-fillings with additional steel fibers (columns C-36 and SQ-11) and reinforcement bars (column SQ-14).

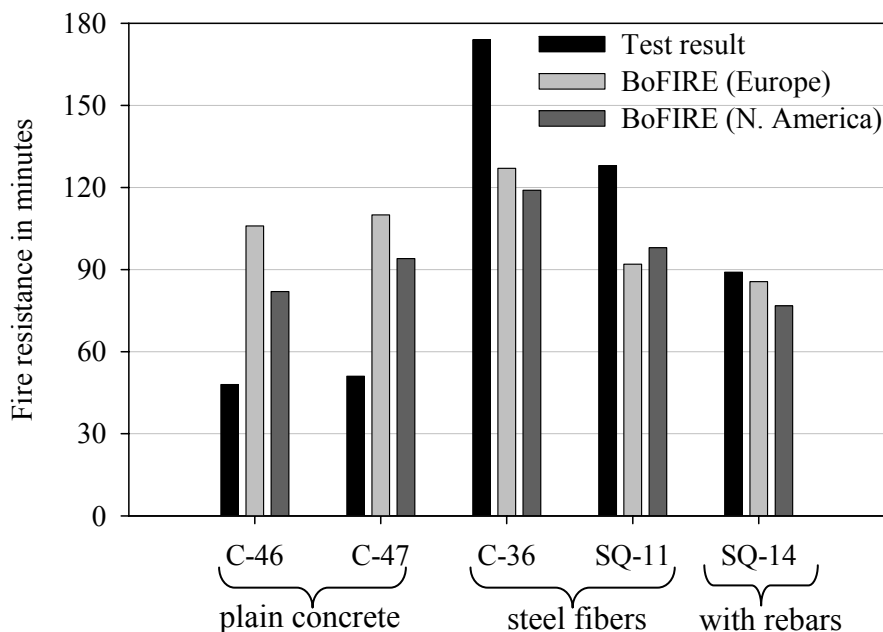


Fig. 4 – Comparison between tested and calculated fire resistance.

The divergence between computed and recorded fire resistance period for mere HSC-filling is attributed to local failure of the columns. Due to cracking of the concrete, the cross-sectional load-bearing capacity is significantly decreased, which causes failure. As the program BoFIRE does not take such effects into account, it might be reasonable to establish a three-dimensional model for this problem in future. Nevertheless, by comparison to the recorded test data it is examined if the distribution of temperatures derived from the computer program BoFIRE is sufficient.

For this purpose, the points at which temperatures are measured in BoFIRE are arranged according to the location of the test thermocouples. At the example of column C-46 with plain HSC-filling, the measured and calculated temperatures according to the HSC material properties defined in the Eurocode 2, part 1-2¹ are presented in Figure 5. A moisture content of 10% of the concrete weight is taken. The comparison ends after 48 minutes since the column fails. Concerning measure point MP 2, the resulting BoFIRE temperatures stand in good agreement with the recorded temperatures. As regards MP 1 in the center of the column, a maximum difference between computed and measured temperatures of approximately 29°C has to be noticed. However, these slight differences cannot be seen as the reason for the high overestimation of the fire resistance of the HSS steel columns with mere HSC-filling.

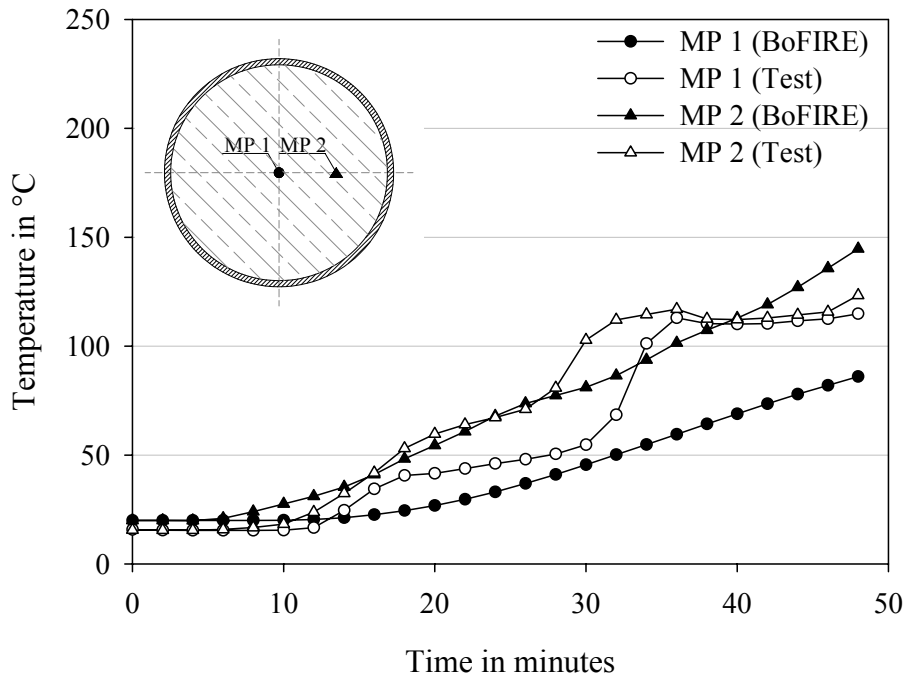


Fig. 5 – Recorded and calculated temperatures for column C-46 according to material properties defined in Eurocode 2, part 1-2¹.

Moreover, it is interesting to study the influence of the moisture content u on the temperature field and the fire resistance period. It is evident from Figure 6 that the computed temperatures for MP 1 decrease with an increasing moisture content u . The difference between ratios of $u=0\%$ and $u=10\%$ already totals to about 120°C after 48 minutes and hence influences the fire resistance period. For example, the fire resistance periods for $u=0\%$ and $u=10\%$ are 89 minutes and 110 minutes, respectively. The results for the moisture content of $u=10\%$ stand in best accordance with the measured temperatures.

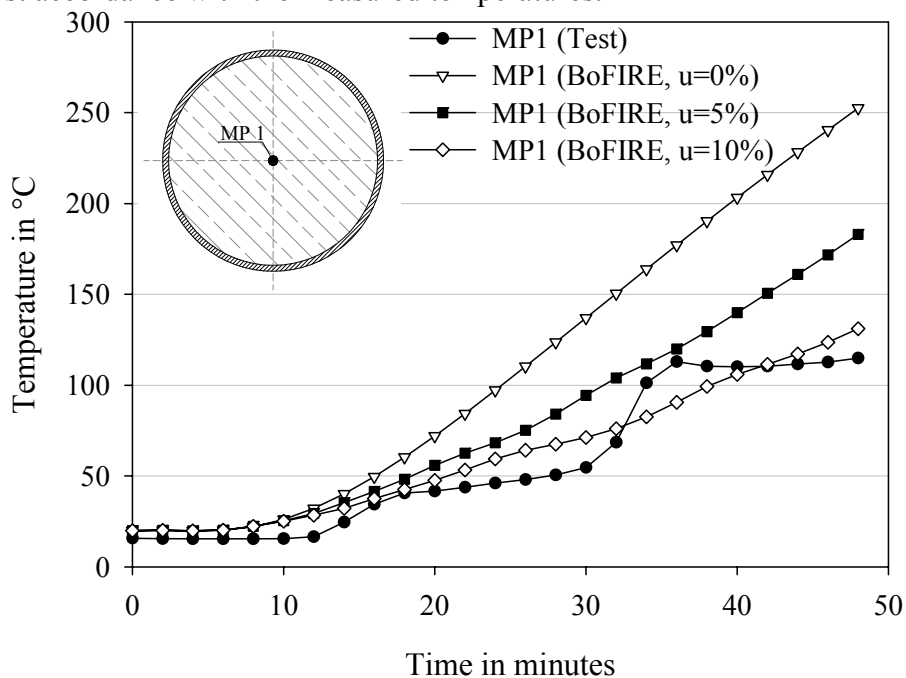


Fig. 6 – Recorded and calculated temperatures for column C-46 with varying moisture content u (calculated with material properties defined in Eurocode 2, part 1-2¹).



For a comparison between the European and North American material properties, the computed temperatures for column SQ-14 (reinforced with bars) are presented in Figures 7 and 8. It becomes clear that the use of the European material properties leads to more realistic cross-sectional temperatures for this example. In addition, the prediction of the fire resistance period stands in very good accordance with the real fire endurance.

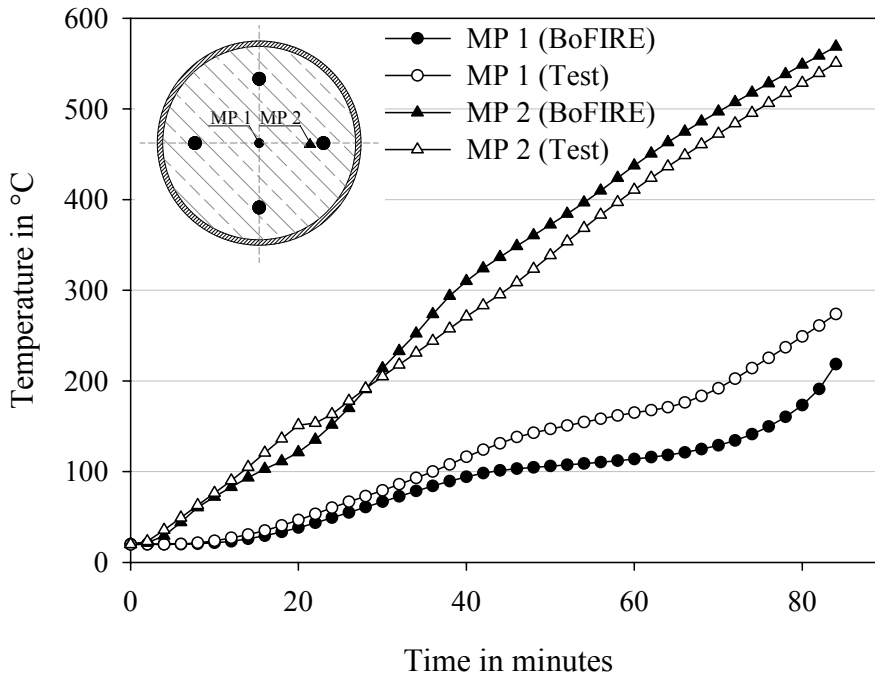


Fig. 7 – Recorded and calculated temperatures for column SQ-14 according to material properties defined in Eurocode 2, part 1-2¹.

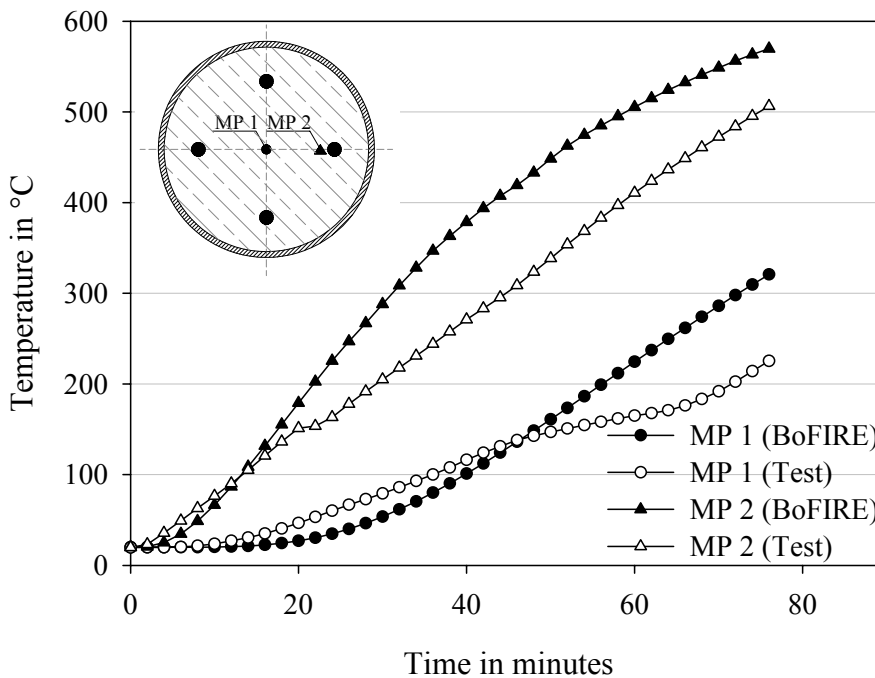


Fig. 8 – Recorded and calculated temperatures for column SQ-14 according to North American material properties^{2,3}.



On the whole, it can be concluded that the calculation of the temperature field with the program BoFIRE is appropriate. Therefore the great difference between tested and computed fire resistance period of plain HSC-filling must be due to micro cracking (which leads to faster loss of strength with temperature) and to spalling. To clarify this question, a comparison of the tested axial deformations between the column with plain HSC-filling C-46, the bar reinforced HSS steel column SQ-14 and the fiber reinforced column SQ-11 is drawn in Figure 9.

Apparently, the general load-bearing behavior is the same for these columns: In the early stages of fire exposure, the load share of the steel part increases significantly since it expands faster than the concrete core. After approximately 20 minutes, the load has to be carried by the concrete core in order of the decreased yield strength of the steel part leading to contraction of the whole column and finally to failure⁴. As it can be seen in Figure 9, the type of concrete-filling influences the contraction phase. The decline is more gradual for both reinforced columns, namely SQ-11 and SQ-14, whereas the failure occurs suddenly for column C-46 with plain HSC-filling. The latter is due to the missing reinforcement resulting in cracks in the concrete core in the local buckling zone. In case of load eccentricities, the load cannot be carried any more¹².

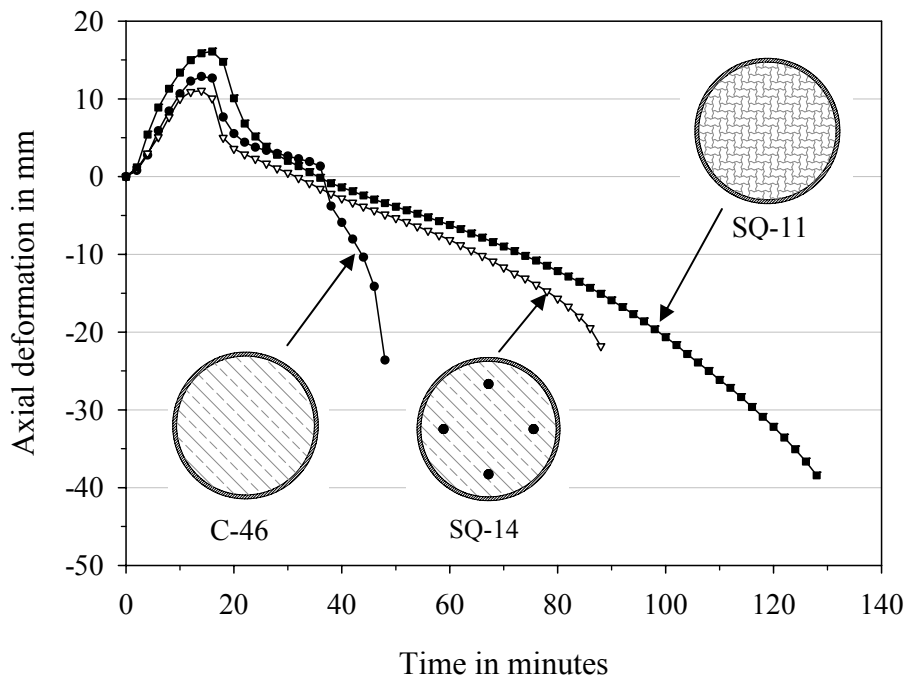


Fig. 9 – Axial deformations recorded in test for specimens C-46, SQ-11 and SQ-14.

Apart from the former investigation, the results of the numerical simulation with the program BoFIRE are also compared to the results derived from the simplified Method A. It is clear that the latter is in particular advantageous for HSS steel columns with mere HSC-filling, given by the specimens C-46 and C-47, as the results stand in far better accordance with the test results than the results calculated with BoFIRE. Contrary to this, the BoFIRE results are more realistic for the other specimens with steel fibers (columns C-36 and SQ-11) and reinforcement bars (column SQ-14).



6. CONCLUSIONS

The temperature field established on the basis of implemented material properties can be seen as sufficient. However, the carried out investigations show that current North American and European material properties are not reliable in predicting the fire resistance period of HSS columns with mere HSC-filling. The divergence between computed and tested fire resistance can be attributed to cross-sectional failure resulting from micro cracks and spalling. The use of additional steel fibers or reinforcement bars significantly reduces these phenomena, which results in conservative computation of the fire endurance with the computer program BoFIRE.

Investigations on the simplified Method A provided by the advanced Eurocode 2, part 1-2¹ show that the scope of application might be extended to HSC. In addition, it could be worthwhile to take the beneficial effect of HSC-filling with steel fibers into account to gain a more realistic prediction of the fire resistance period. Nevertheless, the investigation is based on a limited number of cross-sections and should be extended to other testing programs. As it is difficult and elaborate to consider phenomena like spalling in numerical programs, simplified approaches like Method A are in particular interesting for HSS steel columns with mere HSC-filling. Based on further fire tests and numerical studies, Method A would provide an efficient and economic engineering device for calculating the fire resistance period.

7. REFERENCES

- [1] European Committee for Standardization (CEN), prEN 1992-1-2 (Eurocode 2), “Design of concrete structures, Part 1-2: General rules – Structural fire design”, 2002.
- [2] Canadian Standards Association, “Code for the Design of Concrete Structures for Buildings (CAN3-A23.3-M94)”, Rexdale, 1994.
- [3] Canadian Standards Association, “Limit States Design of Steel Structures (CAN/CSA-S16-01)”, 2001.
- [4] Kodur, V.K.R., “Performance of high strength concrete-filled steel columns exposed to fire”, Canadian Journal of Civil Engineering 25, pp. 975–981, 1998.
- [5] Lie, T.T. and Kodur, V.K.R., “Fire resistance of steel columns filled with bar-reinforced concrete”, Journal of Structural Engineering 122(1), pp. 30-36, 1996.
- [6] Canadian Standards Association, “Standard Methods of Fire Endurance Tests of Building Construction and Materials (CAN/ULC-S101-M89)”, 1989.
- [7] Kodur, V.K.R. and Sultan, M.A., “Effect of temperature on thermal properties of high-strength concrete”, Journal of Materials in Civil Engineering 15(2), pp. 101-107, 2003.
- [8] European Committee for Standardization (CEN), prEN 1994-1-2 (Eurocode 4), “Design of composite steel and concrete structures, Part 1-2: General rules – Structural fire design”, 2004.
- [9] Schaumann, Peter, “Computation of steel members and frames exposed to fire” (in German: “Zur Berechnung stählerner Bauteile und Rahmentragwerke unter Brandbeanspruchung”), Technisch-wissenschaftliche Mitteilungen Nr. 84-4, Institut für konstruktiven Ingenieurbau, Ruhr-Universität Bochum, Germany, 1984.
- [10] Upmeyer, Jens, “Fire design of partially encased composite columns by ultimate fire loads” (in German: “Nachweis der Brandsicherheit von kammerbetonierten Verbundbauteilen über Grenzbrandlasten”), Institute for Steel Construction, University of Hannover, Issue 19, 2001.



- [11] Kettner, Florian, “Investigations on the load-bearing behavior of composite columns under fire conditions”, Institute for Steel Construction, University of Hannover, 2005 (<http://www.stahlbau.uni-hannover.de/en/veroeffentlichungen> → publications → 2005).
- [12] Kordina, Karl and Klingsch, Wolfram, “Fire resistance of composite columns and of solid steel columns – part I”, Studiengesellschaft für Anwendungstechnik von Eisen und Stahl e.V., Project 35, 1983.
- [13] Cheng, F.-P., Kodur, V.K.R. and Wang, T.-C., “Stress-strain curves for high strength concrete at elevated temperatures”, Journal of Materials in Civil Engineering 16(1), pp. 84-94, 2004.
- [14] Kodur, V.K.R. and Lie, T.T, “Fire performance of concrete-filled hollow steel columns”, Journal of Fire Protection Engineering 7(3), pp. 89-98, 1995.
- [15] Kodur, V.K.R. and McGrath, R., “Fire endurance of high strength concrete columns”, Fire Technology 39(1), pp. 73-87, 2003.
- [16] Kodur, V.K.R., “Fire resistance design guidelines for high strength concrete columns”, ASCE/SFPE Specialty Conference of Designing Structures for Fire, Baltimore, 2003.
- [17] Kodur, V.K.R., “Solutions for enhancing the fire endurance of steel HSS columns filled with high strength concrete”, in Press, AISC Steel Construction Journal, pp. 1-22, 2006.

8. APPENDIX

The following formulae describe the material behavior of HSC with steel fibers at elevated temperatures according to Kodur & Sultan⁷ and are referred to as North American material models, for HSC, in the main text:

8.1 Stress-strain relationship

$$f_c = f'_c \times \left[1 - \left(\frac{\varepsilon_{\max} - \varepsilon_c}{\varepsilon_{\max}} \right)^H \right] \quad \text{for: } \varepsilon_c \leq \varepsilon_{c,\max}$$

$$f_c = f'_c \times \left[1 - \left(\frac{30 \times (\varepsilon_{\max} - \varepsilon_c)}{(130 - f'_{c0}) \times \varepsilon_{\max}} \right)^2 \right] \quad \text{for: } \varepsilon_c > \varepsilon_{c,\max}$$

Where:

$$H = 2.28 - 0.012 \times f'_{c0}$$

$$\varepsilon_{\max} = 0.0018 + (6.7 \times f'_{c0} + 6 \times \theta + 0.03 \times \theta^2) \times 10^{-6}$$

And:

$$f'_c = f'_{c0} \times (1.0625 - 0.003125 \times (\theta - 20)) \quad \text{for: } \theta < 100^\circ\text{C}$$

$$f'_c = 0.75 \times f'_{c0} \quad \text{for: } 100 \leq \theta < 400^\circ\text{C}$$

$$f'_c = f'_{c0} \times (1.33 - 0.00145 \times \theta) \quad \text{for: } \theta \geq 400^\circ\text{C}$$

Such that:

$$0 \leq f'_c \leq f'_{c0}$$

Unit: MPa



8.2 Thermal capacity

The specific heat is the product of thermal capacity and density. A value of 2,535 kg/m³ is assumed for the density of HSC with calcareous aggregates.

$$\begin{aligned}\rho_c \times c_p(\theta) &= 3.81 \times 10^6 && \text{for } 0^\circ\text{C} \leq \theta \leq 400^\circ\text{C} \\ \rho_c \times c_p(\theta) &= (-0.0165 \times \theta + 10.41) \times 10^6 && \text{for } 400^\circ\text{C} < \theta \leq 475^\circ\text{C} \\ \rho_c \times c_p(\theta) &= (0.0079 \times \theta - 1.182) \times 10^6 && \text{for } 475^\circ\text{C} < \theta \leq 625^\circ\text{C} \\ \rho_c \times c_p(\theta) &= (0.2333 \times \theta - 142.06) \times 10^6 && \text{for } 625^\circ\text{C} < \theta \leq 700^\circ\text{C} \\ \rho_c \times c_p(\theta) &= (-0.1800 \times \theta + 147.25) \times 10^6 && \text{for } 700^\circ\text{C} < \theta \leq 800^\circ\text{C} \\ \rho_c \times c_p(\theta) &= 3.25 \times 10^6 && \text{for } 800^\circ\text{C} < \theta \leq 1000^\circ\text{C}\end{aligned}$$

8.3 Thermal conductivity

$$\begin{aligned}\lambda_c &= 1.80 - 0.0016 \times \theta_c && \text{for } 0^\circ\text{C} \leq \theta \leq 500^\circ\text{C} \\ \lambda_c &= 1.20 - 0.0004 \times \theta_c && \text{for } 500^\circ\text{C} < \theta \leq 1000^\circ\text{C}\end{aligned}$$

8.4 Thermal elongation

$$\begin{aligned}\varepsilon_c(\theta) &= -2.00 \times 10^{-4} + 9 \times 10^{-6} \times \theta && \text{for } 0^\circ\text{C} \leq \theta \leq 700^\circ\text{C} \\ \varepsilon_c(\theta) &= -3.45 \times 10^{-2} + 58 \times 10^{-6} \times \theta && \text{for } 700^\circ\text{C} < \theta \leq 870^\circ\text{C} \\ \varepsilon_c(\theta) &= 1.60 \times 10^{-2} && \text{for } 870^\circ\text{C} < \theta \leq 1000^\circ\text{C}\end{aligned}$$

8.5 Variation of density

$$\begin{aligned}\rho(\theta)/\rho(20^\circ\text{C}) &= 1.003 - 6 \times 10^{-5} \times \theta && \text{for } 0^\circ\text{C} \leq \theta \leq 700^\circ\text{C} \\ \rho(\theta)/\rho(20^\circ\text{C}) &= 2.214 - 1.79 \times 10^{-3} \times \theta && \text{for } 700^\circ\text{C} < \theta \leq 785^\circ\text{C} \\ \rho(\theta)/\rho(20^\circ\text{C}) &= 0.817 - 1.00 \times 10^{-5} \times \theta && \text{for } 785^\circ\text{C} < \theta \leq 1000^\circ\text{C}\end{aligned}$$